

2019-02

Contrasting responses of stomatal conductance and photosynthetic capacity to warming and elevated CO₂ in the tropical tree species *Alchornea glandulosa* under heatwave conditions

Fauset, S::0000-0003-4246-1828

<http://hdl.handle.net/10026.1/12897>

10.1016/j.envexpbot.2018.10.030

Environmental and Experimental Botany

Elsevier

All content in PEARL is protected by copyright law. Author manuscripts are made available in accordance with publisher policies. Please cite only the published version using the details provided on the item record or document. In the absence of an open licence (e.g. Creative Commons), permissions for further reuse of content should be sought from the publisher or author.

Contrasting responses of stomatal conductance and photosynthetic capacity to warming and elevated CO₂ in the tropical tree species *Alchornea glandulosa* under heatwave conditions

Sophie Fauset^{1*}, Lauana Oliveira², Marcos Buckeridge², Christine H. Foyer³, David Galbraith¹, Rakesh Tiwari¹, Manuel Gloor¹

¹ School of Geography, University of Leeds, Leeds, LS2 9JT, UK

² Instituto de Biociências, Universidade de São Paulo, São Paulo, 05508-090, Brazil

³ Centre for Plant Sciences, University of Leeds, Leeds, LS2 9JT, UK

* Correspondence author, Sophie.fauset@plymouth.ac.uk, present address School of Geography, Earth, and Environmental Sciences, University of Plymouth, Plymouth, PL4 8AA, UK

Abstract

Factorial experiments of combined warming and elevated CO₂ are rarely performed but essential for our understanding of plant physiological responses to climate change. Studies of tropical species are particularly lacking, hence we grew juvenile trees of *Alchornea glandulosa* under conditions of elevated temperature (+1.5°C, eT) and elevated CO₂ (+400ppm, eC) in a factorial open top chamber experiment. We addressed three questions: i) To what extent does stomatal conductance (g_s) reduce with eT and eC treatments?; ii) Is there an interactive effect of eT and eC on g_s ?; iii) Does reduced g_s as a result of eT and/or eC cause an increase in leaf temperature?; iv) Do the photosynthetic temperature optima (T_{opt}) and temperature response of

photosynthetic capacities (V_{cmax} , J_{max}) shift with higher growth temperatures? The experiment was performed during an anomalously hot period, including a heatwave during the acclimation period. Our key findings are that: 1) the eT treatment reduced g_s more than the eC treatment, 2) reduced g_s caused an increase in leaf temperatures, and 3) net photosynthesis and photosynthetic capacities showed very high temperature tolerances with no evidence for acclimation to the eT treatment. Our results suggest that *A. glandulosa* may be able to cope with increases in air temperatures, however reductions in g_s may cause higher leaf temperatures beyond those induced by an air temperature rise over the coming century.

Keywords: photosynthesis, climate change, factorial experiment, tropical forest, warming, carbon dioxide, leaf temperature, v_{cmax} , j_{max} , temperature optima, open top chamber, photosynthetic capacity

1. Introduction

Global atmospheric CO₂ concentrations are increasing, as are air temperatures, with both patterns expected to continue in the coming decades. Plants are a critical part of global biogeochemical cycles, at the interface of the atmosphere and the land surface, with forests storing 65% of terrestrial aboveground biomass (Liu et al., 2015). Plants respond to environmental stimuli, with long-term adaptation and short-term acclimation to changes in light, temperature and other conditions. Photosynthesis, evapotranspiration, and respiration are the primary functions of leaves. Our understanding of leaf-level physiology is used to drive vegetation and land surface models, and hence to project future climate. Experimental research on the responses

of forests to elevated CO₂ has been heavily focussed on temperate ecosystems (Leakey et al. 2012) despite tropical forests stocking more carbon than temperate and boreal forests combined (Pan et al. 2011). Similarly, there are very few studies of thermal acclimation on tropical species (Dusenge & Way 2017). Although temperature increases in the tropics are predicted to be smaller than in other regions (e.g. boreal zone, Collins et al. 2013), tropical forests experience much lower diurnal and seasonal variation in temperature than temperate or boreal forests, and over geological time have experienced a relatively stable climate, potentially reducing the acclimation potential of tropical tree species (Janzen 1967, Dusenge & Way 2017). Investigating the responses of tropical tree species to temperature and CO₂ is therefore a research priority.

Increasing air temperatures and atmospheric CO₂ concentrations lead to changes in stomatal conductance (g_s) over short and long timescales (Way et al., 2015). In the short-term (instantaneous responses), increasing air temperatures typically lead to a reduction in g_s (Way et al., 2015, Slot & Winter 2017a) due to stomatal closure with increasing vapour pressure deficit (D), which prevents excessive water loss under high evaporative demand. At very high temperatures, g_s may actually increase in order to avoid reaching dangerously high leaf temperatures (Slot et al., 2016, Slot & Winter 2017b, Urban et al., 2017, Drake et al., 2018). Evidence of acclimation of g_s to higher temperatures in trees over the long-term is varied, however some species show declines (Way et al., 2015). The instantaneous response of g_s to increased CO₂ is to decrease, which reduces water loss while maintaining a high internal leaf CO₂ concentration (c_i) (Gaastra, 1959). Similarly, under long-term CO₂ enrichment, g_s reduces. Such declines in g_s may increase leaf temperature (T_L) through reduced

76 evaporative cooling (under increased air temperatures, reduced evaporative cooling
77 would also depend on the extent of increased D , Oren et al. 1999). Higher T_L could
78 push leaves beyond their photosynthetic temperature optima (T_{opt}) (Doughty &
79 Goulden 2008, Slot & Winter 2017c), and potentially above their physiological
80 temperature tolerances (O’Sullivan et al., 2017) causing permanent leaf damage under
81 extreme heat conditions (Warren et al., 2011). While the response of g_s to combined
82 elevated CO_2 (eC) and temperature (eT) has rarely been tested (Way et al., 2015,
83 Becklin et al., 2017), experiments on eucalyptus (Ghannoum et al., 2010), douglas-fir
84 (Lewis et al., 2002) and loblolly pine (Wertin et al. 2010) showed little interactive
85 effect; if the two do interact and lead to even greater decreases in g_s , this would
86 increase T_L further.

87
88 Long-term increasing air temperatures and CO_2 concentrations are also predicted to
89 induce changes in net photosynthesis, both directly by impacting biochemical
90 processes and indirectly through changes in g_s . Increases in T_L either directly from
91 increased air temperatures or indirectly from a long-term reduction in g_s could shift
92 the leaf beyond T_{opt} , leading to reductions in photosynthesis. Some experimental
93 studies have shown partial photosynthetic acclimation to increasing temperatures
94 through increases in T_{opt} (Yamori et al., 2014, Slot & Winter 2017b), which could
95 occur due to alterations in membrane fluidity, expression of heat shock proteins, and
96 production of greater quantities of Rubisco activase or a heat-stable Rubisco activase
97 (Yamori et al. 2014). These changes would lead to altered temperature responses of
98 the photosynthetic capacities V_{cmax} (maximum rate of carboxylation) and J_{max}
99 (maximum rate of electron transport). A recent study of four tropical tree species
100 showed that g_s rather than V_{cmax} or J_{max} limited net photosynthesis beyond T_{opt} (Slot &

Winter 2017a), and hence a change to the temperature (or D) response of g_s could also be important for shifts in T_{opt} . Photosynthetic capacities are also influenced by growth CO_2 concentrations. Under high CO_2 , Rubisco concentrations typically reduce and hence V_{cmax} declines (Way et al. 2015). Decreases in g_s (as a consequence of increased air temperature or CO_2) lead to reduced c_i which can reduce assimilation. Under high CO_2 concentrations, this effect could be limited if c_i remains above the Rubisco limited portion of the $A-c_i$ curve, however the downregulation of V_{cmax} commonly observed results in plants still being Rubisco limited even at high CO_2 (Ainsworth & Rogers 2007) and hence reduced g_s could still reduce assimilation (Way et al., 2015).

The effect of decreased conductance on T_L is well understood biophysically (Jones 1992) and is expected to influence T_L under elevated CO_2 (Drake et al. 1997), as has been shown in a small number of experiments (e.g. Siebke et al. 2002, Sigut et al. 2015). However, this effect has not been investigated in any tropical species. Furthermore, because T_L and, to a lesser extent, g_s show high temporal variation with changing microclimate (e.g. Fauset et al., 2018), to fully investigate the effect of altered g_s as a response to elevated temperature and CO_2 it is necessary to measure T_L and microclimate with a high temporal resolution.

In this study, we address the following questions using a factorial eT x eC open top chamber experiment with juveniles of tropical tree species *Alchornea glandulosa* (Poepp. & Endl) (Euphorbiaceae): i) To what extent does g_s reduce with elevated temperature (eT) and elevated CO_2 (eC) treatments?; ii) Is there an interactive effect of eT and eC on g_s ?; iii) Does reduced g_s as a result of eT and/or eC cause an increase in T_L ?; iv) Do the photosynthetic temperature optima (T_{opt}) and temperature response

of photosynthetic capacities (V_{cmax} , J_{max}) shift with higher leaf temperatures? *A. glandulosa* is a pioneer species often found, but not restricted to, riverine environments (Pascotto 2006), distributed in the Atlantic forest, western Amazon/Andes and central America (GBIF Secretariat 2017), with over 100,000,000 individual trees estimated to occur in the Amazon (ter Steege et al., 2013). It is utilized as a timber species, produces medicinal compounds and is used for reforestation in the Atlantic forest region. The fruits of this tree are an important food source for birds (Pascotto 2006). This species was also selected because leaf temperature and stomatal conductance field data for congeneric species *Alchornea triplinervia* were available from the Atlantic forest (Fauset et al., 2018).

2. Methods

2.1 Experimental setup

The study was carried out at the University of São Paulo from February to March 2017 (23.56° S, 46.73° W, elevation 760 m). *Alchornea glandulosa* seedlings were sourced from a local plant nursery where they were germinated in shade houses before growing for 12 months outside.

The seedlings were moved to the glasshouse in September 2016 and in November transferred into containers (4l PVC pots with one plant per plot). Hoagland fertilizer solution was added every 2 weeks. The experiment was conducted using four polycarbonate open top chambers (OTCs) with modifications (Aidar et al., 2002) located within the glass house. The four treatments were: i) control (aTaC), ii)

elevated CO₂ (ambient temperature, 800 ppm CO₂, aTeC), iii) elevated temperature (temperature 1.5°C above ambient, ambient CO₂, eTaC), and iv) elevated CO₂ and elevated temperature (temperature 1.5°C above ambient, 800 ppm CO₂, eTeC). Each chamber had an air inlet at the base with a fan, and a spiral heater and/or CO₂ gas inlet was present depending on the treatment (Figure S1). Temperature within the chamber was thermostatically controlled using RICS software (Remote Integrated Control System) with the heater switched on or off to maintain a higher temperature than the unheated chambers. No attempt was made to control for differences in D due to temperature treatments as increases in temperature would be associated with increases in D under future conditions assuming no change in relative humidity. CO₂ was passively added to the eC treatments through the use of pressurized CO₂ cylinders. The CO₂ concentrations of the eC chambers was monitored daily and the flow into the chambers altered at a valve if the concentration decreased. Further details of the experimental design can be found in Aïdar et al., 2002 and de Souza et al. (2008). Ten seedlings were placed into each chamber on 1 February 2017 and allowed to acclimate for one month before measurements began. Vertical height of each seedling was recorded prior to placement in the OTCs, and placement of seedlings into OTCs was stratified to ensure an even spread of vertical heights.

2.2 Microclimate measurements

Within each OTC air temperature (T_A), relative humidity (h) and CO₂ concentration were measured at 5 min intervals (Testo 535, Testo Inc., Flanders, NJ, USA). An additional T_A sensor (107 thermistor, Campbell Scientific) recorded air temperature every 10 s inside each chamber.

176

177 2.3 Physiological Measurements

178

179 2.3.1 Leaf temperature and leaf surface PAR

180 The eight healthiest of the ten seedlings in each chamber were selected for
181 measurement of leaf temperature. On each selected seedling, one fully expanded
182 healthy leaf was chosen (typically the fourth or fifth newest leaf). These leaves were
183 formed inside the glass house but prior to movement of the seedling into the OTCs.
184 Prior to selection, we verified that the leaves were photosynthetically active. A two-
185 junction thermocouple (copper-constantan, type T) that measured leaf-to-air
186 temperature difference (ΔT_L) was attached to the abaxial surface of each sample leaf
187 using a piece of breathable tape (Transpore, 3M, St. Paul MN) following the protocol
188 of Fauset et al. (2018). One thermocouple was used per leaf. Absolute leaf
189 temperatures (T_L) were calculated from ΔT_L and T_A in each chamber measured by the
190 thermistors. A photosynthetically active radiation (PAR) sensor built to the
191 specification of Fielder & Comeau (2000) was positioned adjacent to each sample leaf
192 at the same angle and orientation. PAR sensors were calibrated against a quantum
193 sensor (LightScout, Spectrum Technologies, Aurora, Illinois). ΔT_L and leaf surface
194 PAR were monitored continuously at 10 s measuring frequency between 24 February
195 – 15 March 2017 using two CR800 data loggers and two AM16/32 multiplexers
196 (Campbell Scientific). Measurements of some leaves were terminated between 10 and
197 15 March. See Fauset et al. (2017, 2018) for further details of these sensors.

198

199 2.3.2 Stomatal Conductance

Stomatal conductance (g_s) of each leaf temperature sample leaf was measured under growth conditions inside the chambers on 19 occasions over six days (including four days where g_s of each leaf was measured at least four times, 28 February – 7 March 2017) using an SC-1 porometer (Decagon). For each time point, two measurements of g_s were recorded, one from either side of the midrib, and the mean value was used for analysis.

2.3.3 Photosynthetic measurements

The temperature response of photosynthesis was measured using a LI-COR 6400XT portable photosynthesis measurement system (LI-COR, Nebraska). Data were collected from 10 – 18 March 2018. Light response curves on 3 leaves showed saturating photosynthesis at $800 \mu\text{mol m}^{-2} \text{s}^{-1}$ PAR (Figure S2), hence all measurements were taken at $800 \mu\text{mol m}^{-2} \text{s}^{-1}$ PAR using the standard red-blue LED light source. Note that the glasshouse roof was made of a diffusing plastic which reduced the incoming PAR by c. 60 % compared with the outside, and leaf level PAR reached c. $800 \mu\text{mol m}^{-2} \text{s}^{-1}$, varying with leaf angle and orientation. Three seedlings from each OTC were selected for photosynthesis measurements and the leaf measurements were performed on the same leaf as leaf temperature monitoring. Two sets of measurements were made, net photosynthesis-temperature curves ($A-T_L$ curves where net photosynthesis at saturating light intensity is measured at different temperatures), and $A-c_i$ curves (where net photosynthesis at saturating light intensity is measured at different CO_2 concentrations) at three different temperatures. $A-T$ curves were run with the CO_2 concentration of the relevant OTC (either 400 or 800 ppm CO_2) and assimilation was measured at leaf chamber temperatures of 20, 25, 27, 29, 31, 33, 35 and 40 °C, with 5 measurements recorded at each temperature after the

photosynthetic rate and g_s had stabilized. Measurements at 20, 30 and 35 °C were supplemented using the relevant measurements from the $A-c_i$ curves. $A-c_i$ curves used the following sequence of CO₂ concentrations (ppm); 400, 200, 100, 50, 400, 600, 800, 1200, 1500, 2000. $A-c_i$ curves were performed at three temperatures, 20, 30, and 35 °C, and each curve was performed twice for each leaf on either side of the midrib. For all measurements, h was maintained as close as possible to 50 % using a combination of desiccant and adjusting the air flow rate; it was difficult to maintain this h at leaf temperatures above 37 °C (on average 46 %, minimum values were 40 %). The temperature of the chamber was mostly controlled using the inbuilt temperature control system. In addition, for most of the measurements the sensor head was placed inside a specially designed temperature control chamber to enable better control of the chamber temperature (Yepes Mayorga 2010). The temperature control box was switched off during measurements but was used to aid the change of chamber temperature between measurements. Measurements were made at an atmospheric pressure in the greenhouse of 92.6 kPa.

2.3.4 Plant growth

Vertical height (from soil surface) and number of leaves of each seedling was measured three times (1 and 21 February, and 16 March). On the latter two measurement days, the length of the seedling from the soil surface to the end of the longest branch was also recorded, and on 16 March the total plant length including all branches was recorded.

2.4 Data analysis

Differences in microclimate between OTCs (air temperature, CO₂ concentration, h and D) were tested using ANOVA and Tukey post-hoc test.

The effects of the warming and the elevated CO₂ treatments on g_s (porometer measurements pooled from all times of day) were tested using two-way ANOVA with a mixed effects model with leaf as a random factor to account for multiple measurements of the same leaves (function ‘lme’ of the R package nlme, Pinheiro et al. 2017). To investigate the response of g_s to microclimate variables and under different treatments, all possible models of PAR and leaf-to-air vapour pressure deficit D_L (where leaf temperature was taken from thermocouple data), with interactions with CO₂ treatment and warming treatment were compared using AIC to select the best model with the function ‘dredge’ in R package MuMIn (Bartoń 2017). Again, a linear mixed effect model with leaf as a random factor was used to account for multiple measurements of the same leaf/seedling. A quadratic effect of time was also included in the model to account for diurnal changes in g_s not directly linked to PAR, temperature or D_L . R^2 for mixed-effects models are given using as the marginal pseudo R^2 that accounts for fixed factors only rather than the conditional pseudo R^2 which also accounts for random effects (Nakagawa & Schielzeth 2013) unless otherwise stated; R^2 values for mixed effects models were calculated using the function provided in the R package MuMIn. We also estimated the g_l parameter of the optimal stomatal conductance model (Medlyn et al. 2011, Lin et al. 2015) from the A-T_L curve data collected with the LI-COR 6400.

$$g_s = 1.6 \left(1 + \frac{g_l}{\sqrt{D}} \right) \frac{A}{C_a}$$

where C_a is the atmospheric CO₂ concentration in the leaf chamber. The model was fit for each leaf, and the g_l parameter was compared between chambers using ANOVA.

275

276 Because leaf temperatures are strongly influenced by microclimate (Jones 1993,
277 Fauset et al. 2018), to assess the influence of treatment on T_L it is necessary to
278 compare T_L within microclimatic envelopes. We subsetting the data into envelopes
279 based on leaf-level PAR, chamber air temperature and D . The data was split into low
280 ($100 - 200 \mu\text{mol m}^{-2} \text{s}^{-1}$), medium ($400 - 500 \mu\text{mol m}^{-2} \text{s}^{-1}$) and high ($700 - 800 \mu\text{mol}$
281 $\text{m}^{-2} \text{s}^{-1}$) PAR, and low ($28 - 30^\circ\text{C}$, $1 - 2 \text{ kPa}$), medium ($33 - 35^\circ\text{C}$, $2 - 3 \text{ kPa}$), and
282 high ($38 - 40^\circ\text{C}$, $3 - 4 \text{ kPa}$) air temperature and D . An unanticipated effect of the
283 switching on and off of the heater in the warmed chambers was a cycle in leaf
284 temperature. This was particularly clear at night, but also occurred during the day.
285 When the heater was switched on, the ΔT_L became more negative as the air heated
286 faster than the leaf (Figure S3). The ΔT_L then rose to reach an equilibrium
287 temperature. Because of this cycle in the ΔT_L data, it was not possible to compare leaf
288 temperatures directly between the ambient and heated chambers, and hence direct
289 comparisons on ΔT_L were only made between CO_2 treatments within temperature
290 treatments.

291

292 The temperature response of photosynthesis is typically modelled as a parabolic curve
293 which provides a T_{opt} parameter (e.g. Robakowski et al. 2012). However, as no
294 evidence of a decline of A with increasing T_L was found (see section 3.4), we could
295 not use the parabolic curve to find T_{opt} (Fig. S4) which was beyond the range of our
296 measurements. Hence, a linear mixed effect model with leaf as a random factor was
297 used to test the relationship between A and T_L . As for stomatal conductance we
298 selected the best model based on AIC from all possible models, here including T_L as a
299 continuous fixed effect and interactions with CO_2 treatment and warming treatment.

300

301 V_{cmax} and J_{max} were estimated for each leaf and each temperature from the $A-c_i$ curve
302 using the Farquhar-von Caemmerer-Berry model using the R package plantecophys
303 (Duursma 2015). For some curves (six for J_{max} and one for V_{cmax} , all at 20 °C), the
304 parameters could not be adequately estimated and estimates were not used. Of the
305 remaining fits, the root mean square error ranged 0.18 – 1.57 $\mu\text{mol m}^{-2} \text{s}^{-1}$. The
306 temperature responses of V_{cmax} and J_{max} were modelled using the Arrhenius function
307 (Medlyn et al. 2002)

308

309
$$f(T_k) = k_{25} \cdot \exp\left(\frac{E_a(T_k - 298)}{(298RT_k)}\right)$$

310

311 where k_{25} is the value of V_{cmax} or J_{max} at 25 °C, E_a is the activation energy (kJ mol^{-1}),
312 T_k is the leaf temperature (°K) and R is the universal gas constant ($8.314 \text{ J mol}^{-1} \text{ K}^{-1}$).
313 The parameters were fit using non-linear least squares (R function nls). This function
314 was fit separately for each chamber, and significant differences in parameter estimates
315 were tested by comparing the 95 % confidence intervals (following Varhammar et al.
316 2015). A peaked Arrhenius function was not used as the data did not show a decline
317 in V_{cmax} or J_{max} at high temperatures.

318

319 **3. Results**

320

321 *3.1 Microclimate over the study period*

322

323 The experimental period coincided with an anomalously hot summer in São Paulo
324 city including a 4 day heatwave (Figure 1). Using the definition of a heatwave from

Russo et al. (2015) as ≥ 3 consecutive days where the maximum temperature exceeds the 90th percentile of maximum temperatures from a monthly window for the period 1981-2010, and climate data for the Mirante de Santana weather station (INMET), a four day heatwave period occurred (maximum temperatures above 32.3 °C) in mid-February (Figure 1, Figure S5). The heatwave occurred during the acclimation period but before the initiation of data collection. During this time the maximum daily air temperatures within the OTCs exceeded 45 °C (Figure 1).

Mean daily temperatures within the OTCs over the acclimation and measurement periods were significantly different between chambers ($F = 5.4$, $P = 0.001$, ANOVA, Figure 2a). Temperatures were significantly lower in the aTeC treatment (28.8 ± 2.3 °C mean \pm SD) than the eTeC treatment (30.4 ± 2.3 °C), however the difference between aTaC (29.0 ± 2.2 °C) and eTaC (30.3 ± 2.4 °C) was marginally insignificant ($P = 0.07$, Tukey post-hoc test, Figure 1a). Mean daily CO₂ concentration was significantly higher in the aTeC and eTeC treatments (829.9 ± 71.6 ppm and 836.7 ± 70.6 ppm, respectively, Figure 1b) than the ambient CO₂ treatments, however the concentration in the eTaC chamber (399.0 ± 8.9 ppm) was significantly lower than the aTaC chamber (459.2 ± 12.2 ppm). Relative humidity also varied by treatment with lower values in the elevated CO₂ treatments (Figure 2c), and D was higher in elevated temperature treatments, significantly so for eTeC (Figure 2d).

3.2 Stomatal Conductance

Analysing g_s data with measurements at all times of day pooled, g_s was significantly lower under the elevated temperature treatments ($P = 0.0001$, mixed effects model

with leaf as a random factor), with no significant effect of CO₂ treatment (Figure 3).

Conductance was highest in the control treatment and similarly low in both elevated

temperature treatments, with an intermediate g_s in the aTeC treatment (Figure 3).

The best mixed effects model of g_s accounting for microclimate and diurnal changes

included time of day, PAR, D_L , and interactions between D_L , warming treatment and

CO₂ treatment (Figure 4, Table 1). The overall pseudo marginal R^2 of the model was

0.38. If the random effect of leaf is also accounted for, the pseudo conditional R^2

increases to 0.67 showing that there is high leaf-to-leaf variation in g_s (Supplementary

Figure 6). Interaction plots (Figure 4) of the model show that the relationship between

g_s and D_L was weak (with no significant effect of D_L alone, Table 1) and varied

between treatments (interactions between heat treatment and D_L , and heat treatment,

CO₂ treatment and D_L were significant, Table 1). Under the aTeC and eTeC

treatments g_s was fairly invariant with D_L , whilst under the eTaC treatment g_s

declined with D_L and under the control aTaC treatment g_s increased with D_L .

However, there is large scatter in the data (Figure 4, Figure S6).

The parameter g_l (inversely proportional with the carbon cost of transpiration and

hence low when a plant is conservative in its water use) estimated from the A-T_L

curves did not show any significant differences between chambers, despite a lower

mean for the eTaC chamber (Figure 5).

3.3 Observed Leaf Temperatures

Diurnal patterns of average ΔT_L , T_L , PAR and D are shown for all chambers in Figure 6 based on the period 24 February – 15 March 2017. There are differences in the patterns of average ΔT_L for each chamber (Figure 6c,d), and these patterns are linked to the patterns of average PAR (Figure 6e,f). In order to properly compare the leaf temperatures between different leaves and chambers, the varying microclimate needs to be accounted for.

Mean ΔT_L values were not significantly different between elevated and ambient CO₂ within the warming treatment under any specified microclimate (Figure 7, eTeC versus eTaC). In contrast, under the majority of microclimates tested ΔT_L values were significantly higher in the elevated CO₂ treatment compared to the ambient CO₂ treatment when under ambient temperatures (Figure 7, aTeC versus aTaC). The microclimate conditions under which no significant differences were found were both in the high PAR category where there were much fewer data points, and the pattern in the data was similar to other microclimates. The extent of the difference in ΔT_L between aTaC and aTeC increased under increasing air temperature and increasing PAR, with a difference of 2.8 °C under high PAR and high air temperature. Analysing the data for T_L rather than ΔT_L produced the same results (data not shown).

3.4 Photosynthetic Temperature Response Curves

Despite measuring photosynthesis at leaf temperatures up to 40 °C, there was no evidence of reaching T_{opt} as A continued to increase with T_L for the majority of leaves (Figure 8). Consequently, estimation of T_{opt} was not attempted and linear models were used to analyse the A - T_L curves. There was no significant effect of temperature

treatment, however T_L , CO₂ treatment and their interaction were included in the best model. A (measured at the growth CO₂ concentration) was higher and the slope of the A - T relationship was steeper under the elevated CO₂ treatments (Figure 8). The marginal pseudo- R^2 of the model was 0.53, and all model terms (T_L , CO₂ treatment and their interaction) were significant (Table 2).

3.5 Temperature Responses of V_{cmax} and J_{max}

As for A , both V_{cmax} and J_{max} increased with measurement temperature (Figure 9) and no optimum temperature was found within the measurement range (20 – 35 °C). V_{cmax} varied ranged 6.1 – 51.8 $\mu\text{mol m}^{-2} \text{s}^{-1}$ and J_{max} ranged 16.3 – 46.3 $\mu\text{mol m}^{-2} \text{s}^{-1}$ with standard errors ranging 0.097 – 6.88 $\mu\text{mol m}^{-2} \text{s}^{-1}$ for V_{cmax} and 0.29 - 2.76 $\mu\text{mol m}^{-2} \text{s}^{-1}$ for J_{max} . The higher SE values correspond with higher parameter values. Temperature treatment had no significant effect on either of the two variables, however V_{cmax} was lower and the temperature response of V_{cmax} was weaker (lower activation energy) under elevated CO₂, with significant differences between eTaC and eTeC treatments (Figure 9, Table 3). The ratio of J_{max}/V_{cmax} decreased with increasing temperature (30 - 35 °C, not sufficient J_{max} data at 20°C), and was significantly higher in the elevated CO₂ treatment (Figure S7).

3.6 Seedling growth

There were no significant effects of treatment on seedling size at any time point during the experiment (vertical height, total branch length, number of leaves, Figure S8).

4. Discussion

In this study we present a factorial elevated temperature and elevated CO₂ experiment with juveniles of a tropical pioneer species. The study was performed under high temperature conditions including a heatwave during the acclimation period (Figure 1). Our key findings are i) that the elevated temperature treatment had a stronger influence on g_s than elevated CO₂ (Figure 3, Table 1), ii) that reduced g_s caused a change in leaf temperatures (Figure 7), iii) that net photosynthesis and photosynthetic capacities show very high temperature tolerances with no evidence for acclimation to the elevated temperature treatment (Figure 8), and iv) that there was no interactive effect of temperature and CO₂ treatment on g_s (Figure 3, Table 1)

4.1 Temperature and CO₂ impacts on stomatal conductance

As expected, g_s declined in the eC treatments compared with the control, as has been shown in many other studies. Here we find a 21.2 % reduction (95% CI 10.6 – 30.2 % based on bootstrapping) in our aTeC treatment compared with the control (Figure 2). In forest free air CO₂ enrichment (FACE) experiments with CO₂ elevated by 200 ppm g_s declines on average by *c.* 20 % (Ainsworth & Rogers 2007), with stronger declines in angiosperm than gymnosperm species (Brodribb et al. 2009). Past chamber experiments performed on angiosperm trees with a doubling of CO₂ show an average g_s reduction of *c.* 18 % (from data in Saxe et al. 1998). Our data therefore shows consistency with species from other biomes, but with few tropical species included in existing studies. The literature on tropical species shows wide variation (Berryman et

al. 1994, Goodfellow et al. 1997, Liang et al. 2001, Leakey et al. 2002, Khurana & Singh 2004, Cernusak et al. 2011, Dalling et al. 2016, Wahidah et al. 2017). Data from eight publications covering 22 tropical angiosperm species with CO₂ enrichment in the range 300-400 ppm showed an average change in g_s of 28.6 ± 18.4 % SD reduction. One species (*Chrysophyllum cainito*) showed a very small increase (Dalling et al. 2016), and the largest reduction of 61 % was shown by *Inga punctata* (Cernusak et al. 2011). Hence, the reduction we observed was below average but well within the range of observations of other tropical species in experiments.

A limitation of our experiment and its comparability with other studies is the short duration of exposure to the treatments. We measured the physiological responses on leaves formed before initiation of the experiment, which had been exposed to the treatments for *c.* 5 weeks. As stomatal properties (e.g. density) often differ on leaves formed in high CO₂ environments (Saxe et al. 1998), there could potentially be greater changes than we observed, had new leaves formed. Whilst this is quite possible, the long-term response of g_s to CO₂ is typically similar to the short term response (Way et al. 2015), and hence while the mechanism of reduced g_s may be different in short and long-term studies, the g_s may be similar. However, a caveat to our results is that to truly observe the acclimation of leaves to the treatments, longer acclimation periods and production of new leaves is necessary.

The observed responses of g_s to elevated temperature vary considerably in the few studies available (Way et al. 2015). Here we find strong reductions in g_s in the temperature treatments with a 49.6 % (95% CI 42.2 – 56.5 %) reduction under the eTaC treatment and 53.0 % (95% CI 52.9 – 58.3 %) reduction in the combined eTeC

treatment, although we did not find any significant difference between treatments for the g_l parameter value. This may be because the Medlyn et al. (2011) model incorporates the ambient CO₂ concentration, and if the short-term and long term g_s response to CO₂ is the same there would not be a difference. The declines in g_s are not driven purely by higher D_L in the eT chambers as there are significant differences even when D_L is controlled for (Table 1, Figure 4) or when g_s is analysed within a narrow D_L range (data not shown). This shows acclimation of g_s due to higher air temperature and/or D_L (both quantities strongly co-varied) which will reduce water loss from the plants. There were no significant differences in g_s between the eTaC and eTeC treatments, hence the response to the temperature treatment (with significant differences) was stronger than the response to the CO₂ treatment. The result is surprising given the very mixed results in the limited literature on elevated temperature impacts on g_s , and even more so given that in this study the temperature treatment was fairly modest (+1.5 °C) compared to the CO₂ treatment (+ 400 ppm), although the effect of eC on g_s may have been limited by the lack of new leaf development (as stated above). This finding could also be because the ambient temperatures were very hot inside the chambers throughout the experiment and especially during the acclimation phase (Figure 1), which meant that a small increase in air temperature had a large impact, with stomata closing to reduce water loss. An experimental study of gas exchange of *Solanum lycopersicum* (cherry tomato) measured during and following a +14 °C heatwave showed reduced g_s during the heatwave, which remained low when measured 5 days after the heatwave (Duan et al., 2016). Similarly, Duarte et al. (2016) found reduced g_s of *Pseudotsuga menziesii* (Douglas fir) during +12 °C heatwaves which remained when measured one month later. This is somewhat in contrast with recent research suggesting stomata remain

open under very high air temperatures for increased evaporative cooling (Slot et al., 2016, Slot & Winter 2017b, Urban et al., 2017, Drake et al, 2018). Responses are likely to be species specific, with an example of a late successional species reducing g_s under heatwave conditions while a pioneer species showed increased g_s (Vargas & Cordero 2013). However these studies are assessing the instantaneous response of g_s to short-term warming rather than the long-term response. A field study reporting the impact of four months of experimentally elevated temperature on g_s of existing leaves showed a *c.* 25 % reduction with 2 °C temperature increase averaged across six tropical species (Doughty 2011), lower than we observed. However, in contrast to our results for *Alchornea glandulosa*, Yepes Mayorga (2010) found that g_s of *Hymenaea courbaril* was more strongly controlled by elevated CO₂ than elevated temperature in a similar study, as did Ameye et al. (2012) in a study of temperate species *Quercus rubra* and *Pinus taeda* in treatments of elevated by 320 ppm and T_A elevated by 3 °C or with heat waves. Two studies of subtropical/temperate *Eucalyptus* spp. found no difference in g_s of under treatments of CO₂ elevated by 240 ppm and T_A elevated by 3 °C or 4 °C after 15 and 7 months of acclimation respectively (Quentin et al. 2013, Duan et al. 2018). While more studies are needed to see if there is a general pattern for tropical broadleaf species, the results of this study suggest that there could be larger implications of rising temperature than rising CO₂ for water use of at least some species of tropical tree, and even implications of modest temperature rises such as the ambitious aims of the Paris Agreement (UNFCCC 2015).

The g_s dataset also showed a weak relationship with respect to D_L , which varied with treatment (Table 1, Figure 3). Other studies with a congeneric species show that g_s of *A. triplinervia* is more weakly linked to D_L than other measured species (García-

Núñez et al. 1995, Fauset et al. 2018). A weaker relationship between g_s and D_L is expected for low wood density pioneer species compared to species with higher wood density (Lin et al. 2015). In addition, as the species is commonly found in riparian areas (and therefore with access to a good water supply), its lack of stomatal control is not surprising. Our results show that despite a weak instantaneous response of g_s to microclimate, *A. glandulosa* still showed acclimation and reduction in g_s in response to long-term microclimate change. Hence, the short-term response of g_s does not provide information on the long-term response.

4.2 CO_2 impacts on leaf temperature

The lower g_s as a result of elevated CO_2 caused increases in leaf temperatures (Figure 5). The differences in ΔT_L increased with increasing PAR at the leaf surface, and to a lesser extent with increasing air temperature and D . This shows that the differences in leaf temperatures due to CO_2 -altered g_s are more apparent under high thermal stress conditions (high PAR and high air temperature), and therefore that this impact is likely to be stronger under heat waves, which are expected to increase in frequency during the 21st century (Coumou & Robinson 2013). When at high air temperatures, differences in ΔT_L due to reduced g_s could have significant consequences, as seen in observations of premature leaf senescence during a heatwave in a temperate FACE experiment (Warren et al. 2011). While the average differences in ΔT_L between aTaC and aTeC reached 2.8 °C under high light and air temperature, the light conditions were limited by the greenhouse environment which reached only 1000 $\mu\text{mol m}^{-2} \text{s}^{-1}$. Under field conditions where incoming PAR can reach over 2500 $\mu\text{mol m}^{-2} \text{s}^{-1}$ the impact of reduced g_s on ΔT_L could be much higher. Unfortunately due to ΔT_L

fluctuations induced by heating the air (Figure S3) it was not possible to assess the impact of the high temperature treatment compared to the control. Within the two high temperature treatments there were no significant differences in ΔT_L under any microclimate between the elevated and ambient CO₂ treatments, which is expected as they did not show any significant differences in g_s .

4.3 Temperature and CO₂ impacts on photosynthesis

The elevated temperature treatment had no discernible effect on A or photosynthetic capacity and their responses to elevated temperatures. The high temperature tolerance of both A and photosynthetic capacity was marked, with no decline in A found even at 40 °C. Consequently, we were not able to assess shifts in T_{opt} with treatment as T_{opt} was above the maximum temperature under which we performed measurements. It is worth noting that such high leaf temperatures are often considered to be detrimental to photosynthetic functions (e.g. Rubisco activase activity is strongly temperature sensitive with inhibition found above 35 °C [Crafts-Brandner & Salvucci 2000]). Moreover, photosystem II (PSII) activity declines rapidly above temperature thresholds of 41.5 – 50.8 °C (O’Sullivan et al. 2017). However, plants are well adapted to their environment, with temperature thresholds of PSII increasing from arctic to tropical habitats (O’Sullivan et al. 2017), and even increasing thermal tolerance of PSII over very short timescales (days) in response to high temperatures (Drake et al. 2018). Slot et al. (2017c) found that T_{opt} measured in the field in Panama was around the mean maximum daily temperature (30-32 °C) for all 42 species measured, and that, for a smaller sample of four species, it was g_s rather than Rubisco activase, J_{max} , V_{cmax} or light respiration that limited the photosynthetic rates at high

temperatures (Slot & Winter 2017a). In another study, T_{opt} was higher than daily maximum air temperature in moist and wet tropical forest sites in Puerto Rico (Mau et al. 2018). In the case of the *A. glandulosa* seedlings measured here, the mean maximum daily temperature over the acclimation and measurement period was 40 – 42 °C (varying by treatment, Figure 1), matching the minimum potential T_{opt} of 40 °C, and showing tolerance to the high temperatures to which they were exposed. Measurement under higher temperatures would be necessary to find the T_{opt} for these plants. Over the measured temperature range, g_s , V_{cmax} and J_{max} did not decline. Yet, it should also be noted that the rates of A , V_{cmax} and J_{max} were fairly low (c. 3, 40 and 35 $\mu\text{mol m}^{-2} \text{s}^{-1}$ respectively, at the highest values and under ambient CO_2). For example, these are lower than A of 12 – 16 $\mu\text{mol m}^{-2} \text{s}^{-1}$ across 42 Panamanian species (Slot & Winter 2017c) and 5 – 12 $\mu\text{mol m}^{-2} \text{s}^{-1}$ for four species in Puerto Rico (Mau et al. 2018), and V_{cmax} of 70 – 300 $\mu\text{mol m}^{-2} \text{s}^{-1}$ and J_{max} of 80 – 220 $\mu\text{mol m}^{-2} \text{s}^{-1}$ across four Panamanian species (Slot & Winter 2017a), all at their optimum temperatures. The measured rates are also lower than plants in other high temperature environments e.g. five desert species with A ranging 19 – 35 $\mu\text{mol m}^{-2} \text{s}^{-1}$ (Mooney et al. 1981), and Mediterranean cork oak with V_{cmax} and J_{max} both over 150 $\mu\text{mol m}^{-2} \text{s}^{-1}$ (Ghouil et al. 2003). Thus, high temperature tolerance of photosynthetic machinery in *A. glandulosa* may come at a cost of lower photosynthetic rates. An alternative explanation for the low photosynthetic rates is the low light conditions within the greenhouse, with maximum leaf surface PAR of 800-1000 $\mu\text{mol m}^{-2} \text{s}^{-1}$. In the field, maximum PAR is likely to be much higher ($> 2000 \mu\text{mol m}^{-2} \text{s}^{-1}$), and leaves may achieve higher photosynthetic rates. The low light conditions in the greenhouse also have implications for the high temperature tolerance observed. Because at high temperatures photosynthetic biochemistry is under greater stress, there is a greater

need for photoprotection from high incoming radiation. Perhaps under the higher light conditions found in the field, very high temperature tolerance of photosynthesis may be more difficult to achieve. Field studies under high temperature conditions are needed to establish whether the high tolerance we find here also occurs under natural conditions.

As for g_s , the impacts of increased CO_2 followed expectations from previous studies with increased net photosynthesis when measured at growth CO_2 , a steeper slope of A in response to temperature, and downregulation of photosynthetic capacity (Figure 8, 9). The steeper slope is due to the reduction in oxygenation of Rubisco due to higher c_i under elevated CO_2 , which otherwise increases with temperature due to the reduced affinity of Rubisco for CO_2 with higher temperature (Long 1991). The effect of the downregulation can be seen when the temperature response of A is plotted with added points taken from the $A-c_i$ curves at 400 and 800 ppm CO_2 for the elevated and ambient CO_2 treatments respectively, showing that without the downregulation of photosynthetic capacity A would have been higher in the elevated CO_2 treatment (Figure S9).

4.4 Conclusions

This study demonstrates that the tropical tree species *Alchornea glandulosa* shows strong responses of stomatal conductance to elevated temperature and of photosynthetic parameters to elevated CO_2 . While a very high temperature tolerance of photosynthesis was observed in this species, photosynthetic rates were low under the high growth temperatures. These results show that this species will be able to cope

with the predicted atmospheric changes over the coming century. Therefore, it is an appropriate species for reforestation activities, which are planned and ongoing in the Atlantic forest (Rodrigues et al. 2009). More studies of other species are required to determine whether similar results occur in other forest trees.

5. Acknowledgements

We thank Viviane Costa at the Lafieco greenhouse, and Santiago Clerici and David Ashley at the University of Leeds, for considerable assistance with this project. We acknowledge funding from Natural Environment Research Council/NERC (NE/K01644X/1 and NE/N012542/1) and the State of São Paulo Research Foundation/FAPESP (2012/51509-8, 2012/51872-5) as part of the projects ECOFOR and BIODRED and the European Research Council project GEM-TRAIT awarded to Yadvinder Malhi.

6. CRediT Author Statement

Sophie Fauset: Conceptualization, Formal Analysis, Investigation, Writing – Original Draft, Lauana Oliveira: Investigation, Writing – Review & Editing, Marcos Buckeridge: Resources, Conceptualization, Writing – Review & Editing, Christine H. Foyer: Writing – Review & Editing, David Galbraith: Funding Acquisition, Writing – Review & Editing, Rakesh Tiwari: Writing – Review & Editing, Manuel Gloor: Conceptualization, Funding Acquisition, Writing – Review & Editing.

7. References

648 Aidar, M.P.M., Martinez, C.A., Costa A.C., Costa, P.M.F., Dietrich, S.M.C.,
649 Buckeridge, M.S., 2002. Effect of atmospheric CO₂ enrichment on the establishment
650 of seedlings of jatobá, *Hymenaea courbaril* L. (Leguminosae, Caesalpinioideae).
651 Biota Neotropica 2 (1).
652
653 Ainsworth, E.A., Rogers, A., 2007. The response of photosynthesis and stomatal
654 conductance to rising [CO₂]: mechanisms and environmental interactions. Plant Cell
655 Env. 30, 258-270.
656
657 Ameye, T., Wertin, T.W., Bauweraerts, I., McGuire, M.A., Teskey, R.O., Steppe, K.,
658 2012. The effect of induced heat waves on *Pinus taeda* and *Quercus rubra* seedlings
659 in ambient and elevated CO₂ atmospheres. New Phytol. 196, 448-461.
660
661 Bartoń, K., 2016. MuMIn: Multi-Model Inference. R Package version 1.15.16.
662
663 Becklin, K.M., Walker II., S.M., Way, D.A., Ward, J.K., 2017. CO₂ studies remain
664 key to understanding a future world. New Phytol. 214, 34-40.
665
666 Berryman, C.A., Eamus, D., Duff, G.A., 1994. Stomatal responses to a range of
667 variables in two tropical tree species grown with CO₂ enrichment. J. Exp. Bot. 45,
668 539-546.
669
670 Brodribb, T., McAdam, S.A.M., Jordan, G.J., Feild, T.S., 2009. Evolution of stomatal
671 responsiveness to CO₂ and optimization of water-use efficiency among land plants.
672 New Phytol. 183, 839-847.

673

674 Collins, M., Knutti, R., Arblaster, J., Dufresne, J.-L., Fichefet, T., Friedlingstein, P.,
675 ..., Wehner, M., 2013. Long-term climate change: Projections, commitments and
676 irreversibility. In: Climate Change 2013: The Physical Science Basis. Contribution of
677 working group I to the Fifth Assessment Report of the Intergovernmental Panel on
678 Climate Change (eds Stocker, T.F., Qin, D., Plattner, G.-K., Tignor, M., Allen, S.K.,
679 Boschung, J., ..., Midgley, P.M.), pp 1029-1136, Cambridge University Press,
680 Cambridge, UK and New York, USA.

681

682 Cernusak, L.A., Winter, K., Martínez, C., Correa, E., Aranda, J., Garcia, M.,
683 Jaramillo, C., Turner, B.L., 2011. Responses of legume versus nonlegume tropical
684 tree seedlings to elevated CO₂ concentration. *Plant Physiol.* 157, 372-385.

685

686 Coumou, D., Robinson, A., 2013. Historic and future increase in the global land area
687 affected by monthly heat extremes. *Environ. Res. Lett.* 8, 034018.

688

689 Crafts-Brandner, S.J., Salvucci, M.E., 2000. Rubisco activase constrains the
690 photosynthetic potential of leaves at high temperature and CO₂. *Proc. Nat. Acad. Sci.*
691 2000, 13430-13435.

692

693 Dalling, J.W., Cernusak, L.A., Winter, K., Aranda, J., Garcia, M., Virgo, A.,
694 Cheesman, A.W., Baresch, A., Jaramillo, C., Turner, B.L., 2016. Two tropical
695 conifers show strong growth and water-use efficiency responses to altered CO₂
696 concentration. *Annals Bot.* 118, 1113-1125.

697

698 De Souza, A.P., Gaspar, M., da Silva E.A., Ulian, E.C., Waclawovsky, A.J.,
699 Nishiyama Jr., M.Y., ..., Buckeridge, M.S., 2008. Elevated CO₂ increases
700 photosynthesis, biomass and productivity, and modifies gene expression in sugarcane.
701 *Plant Cell Environ.* 31, 1116–1127
702
703 Doughty, C.E., Goulden, M.L., 2008. Are tropical forests near a high temperature
704 threshold? *J. Geophys. Res.* 113, G00B07.
705
706 Doughty, C.E., 2011. An in situ leaf and branch warming experiment in the Amazon.
707 *Biotropica* 43, 658-665.
708
709 Drake, B.G., González-Meler, M.A., Long, S.P., 1997. More efficient plants: A
710 consequence of rising atmospheric CO₂? *Annu. Rev. Plant Phys.* 48, 609-639.
711
712 Drake, J.E., Tjoelker, M.G., Vårhammar, A., Medlyn, B.E., Reich, P.B., Leigh, A.,
713 ..., Barton, C.V.M., 2018. Trees tolerate an extreme heatwave via sustained
714 transpirational cooling and increased leaf thermal tolerance. *Glob. Change Biol.*
715 10.1111/gcb.14037.
716
717 Duan, H., Chaszar, B., Lewis, J.D., Smith, R.A., Huxman, T.E., Tissue, D.T., 2018.
718 CO₂ and temperature effects on morphological and physiological traits of drought-
719 induces mortality. *Tree Physiology* 38, 1138-1151.
720
721 Duarte, A.G., Katata, G., Hoshika, Y., Hossain, M., Kreuzwieser, J., Arneth, A.,
722 Ruehr, N.K. 2016. Immediate and potential long-term effects of consecutive heat

723 waves on the photosynthetic performance and water balance in Douglas-fir. *J. Plant*
724 *Physiology* 205, 57-66.
725
726 Dusenke, M.E., Way, D.A., 2017. Warming puts the squeeze on photosynthesis –
727 lessons from tropical trees. *J. Exp. Bot.* 68, 2073-2077.
728
729 Duursma, R.A. 2015. Plantecophys – an R package for analysing and modelling leaf
730 gas exchange data. *PLoS ONE* 10, e0143346.
731
732 Fauset, S., Gloor, E.U., Aidar, M.P.M., Freitas, H.C., Fyllas, N.M., Marabesi, M.A.,
733 ..., Joly, C.A., 2017. Tropical forest light regimes in a human-modified landscape.
734 *Ecosphere* 8, e02002.
735
736 Fauset, S., Freitas, H.C., Galbraith, D.R., Sullivan, M.J.P., Aidar, P.M., Joly, C.A.,
737 ..., Gloor, M.U., 2018. Differences in leaf thermoregulation and water use strategies
738 between three co-occurring Atlantic forest tree species. *Plant Cell Env.* DOI:
739 10.1111/pce.13208
740
741 Fielder, P., Comeau, P., 2000. Construction and testing of an inexpensive PAR
742 sensor. Ministry of Forests Research Program. Victoria, British Columbia, Working
743 Paper 53/2000.
744
745 García-Núñez C., Azócar, Rada, F., 1995. Photosynthetic acclimation to light in
746 juveniles of two cloud forest tree species. *Trees* 10, 114-124.
747

748 Gaastra P., 1959. Photosynthesis of crop plants as influenced by light, carbon
749 dioxide, temperature, and stomatal diffusion resistance. Mededel
750 Landbouwho Gesch Wageningen 59, 1–68.
751
752 GBIF Secretariat, 2017. *Alchornea glandulosa* Poepp. GBIF Backbone Taxonomy.
753 Checklist Dataset <https://doi.org/10.15468/39omei> (accessed via GBIF.org 9 February
754 2018).
755
756 Ghannoum, O., Phillips, N.G., Sears, M.A., Logan, B.A., Lewis, J.D., Conroy, J.P.,
757 Tissue, D.T., 2010. Photosynthetic responses of two eucalypts to industrial-age
758 changes in atmospheric [CO₂] and temperature. *Plant Cell Env* 33, 1671-1681.
759
760 Ghouil, H., Montpied, P., Epron, D., Ksontini, M., Hanchi, B., Dreyer, E., 2003.
761 Thermal optima of photosynthetic functions and thermostability of photochemistry in
762 cork oak seedlings. *Tree Physiology* 23, 1031-1039.
763
764 Goodfellow, J., Eamus, D., Duff, G., 1997. Diurnal and seasonal changes in the
765 impact of CO₂ enrichment on assimilation, stomatal conductance and growth in a
766 longterm study of *Manigifera indica* in the wet-dry tropics of Australia. *Tree*
767 *Physiology* 17, 291-299.
768
769 Janzen, D.H., 1967. Why mountain passes are higher in the tropics. *Am. Nat.* 101,
770 233-249.
771

772 Jones H.G., 1992. Plants and microclimate. Cambridge University Press, Cambridge,
773 UK.
774

775 Khurana E., Singh, J.S., 2004, Response of five dry tropical tree species to elevated
776 CO₂: impact of seed size and successional status. *New Forests*, 27, 139-157.
777

778 Körner, C., Würth, M., 1996. A simple method for testing leaf responses of tall
779 tropical forest trees to elevated CO₂. *Oecologia* 107, 421-425.
780

781 Leakey, A.D.B., Bishop, K.A., Ainsworth, E.A., 2012. A multi-biome gap in
782 understanding of crop and ecosystem responses to elevated CO₂. *Curr. Opin. Plant*
783 *Biol.* 15, 228-236.
784

785 Leakey, A.D.B., Press, M.C., Scholes, J.D., Watling, J.R., 2002. Relative
786 enhancement of photosynthesis and growth at elevated CO₂ is greater under sunflecks
787 than uniform irradiance in a tropical rain forest tree seedling. *Plant Cell Environ.* 25,
788 1701-1714.
789

790 Lewis, J.D., Lucash, M., Olszyk, D.M., Tingley, D.T., 2002. Stomatal responses of
791 Douglas-fir seedlings to elevated carbon dioxide and temperature during the third and
792 fourth years of exposure. *Plant Cell Env.* 25, 1411-1421.
793

794 Liang, N., Tang, Y., Okuda, T., 2001. Is elevation of carbon dioxide concentration
795 beneficial to seedling photosynthesis in the understorey of tropical rain forests? *Tree*
796 *Physiology* 21, 1047-1055.

797 Lin, Y.-S., Medlyn, B.E., Duursma, R.A., Prentice, I.C., Wang, H., Baig, S., ...,
798 Wingate, L., 2015. Optimal stomatal behaviour around the world. *Nat. Clim. Change*
799 5, 459-464.
800
801 Liu, Y.Y., van Dijk, A.I.J.M., de Jeu, R.A.M., Canadell, J.G., McCabe, M.F., Evans,
802 J.P., Wang, G., 2015. Recent reversal in loss of global terrestrial biomass. *Nat. Clim.*
803 *Change* 5, 470-474.
804
805 Long, S.P., 1991. Modification of the response of photosynthetic productivity to
806 rising temperature by atmospheric CO₂ concentrations: Has its importance been
807 underestimated? *Plant Cell Env.* 14, 729-739.
808
809 Lovelock, C.E., Virgo, A., Popp, M., Winter, K., 1999. Effects of elevated CO₂
810 concentration on photosynthesis, growth and reproduction of branches of the tropical
811 canopy tree species, *Luehea seemannii* Tr. & Planch. *Plant Cell Env.* 22, 49-59.
812
813 Mau, A.C., Reed, S.C., Wood, T.E., Cavaleri, M.A., 2018. Temperate and tropical
814 forest canopies are already functioning beyond their thermal thresholds for
815 photosynthesis. *Forests* 9, doi:10.3390/f9010047.
816
817 Medlyn, B.E., Dreyer, E., Ellsworth, D., Forstreuter, M., Harley, P.C., Kirshbaum,
818 M.U.F., ..., Loustau, D., 2002. Temperature response of parameters of a
819 biochemically based model of photosynthesis. II. A review of experimental data.
820 *Plant Cell Env.* 25, 1167-1179.
821

822 Medlyn, B.E., Duursma, R.A., Eamus, D., Ellsworth, D.S., Prentice, I.C., Barton,
 823 C.V.M., ..., Wingate, L., 2011. Reconciling the optimal and empirical approaches to
 824 modelling stomatal conductance. *Global Change Biol.* 17, 2134-2144.
 825
 826 Mooney, H.A., Field, C., Gulmon, S.L., Bazzaz, F.A., 1981. Photosynthetic capacity
 827 in relation to leaf position in desert versus old-field annuals. *Oecologia*, 50, 109-112.
 828
 829 Nakagawa, S., Schielzeth, H. 2013. A general and simple method for obtaining R²
 830 from generalized linear mixed-effects models. *Methods Ecol. Evol.* 4, 133–142.
 831
 832 Oren, R., Sperry, J.S., Katul, G.G., Pataki, D.E., Ewers, B.E., Phillips, N., Schäfer,
 833 K.V.R., 1999. Survey and synthesis of intra- and interspecific variation in stomatal
 834 sensitivity to vapour pressure deficit. *Plant Cell Env.* 22, 1515-1526.
 835
 836 O’Sullivan, O.S., Heskell, M.A., Reich, P.B., Tjoelker, M.G., Weerasinghe, L.K.,
 837 Penillard, A., ..., Atkin, O.K. 2017. Thermal limits of leaf metabolism across biomes.
 838 *Glob. Change Biol.* 23, 209-223.
 839
 840 Pan, Y., Birdsey, R.A., Fang, J., Houghton, R., Kauppi, P.E., Kurz W.A., ..., Hayes
 841 D. 2011., A large and persistent carbon sink in the world’s forests. *Science* 333, 988-
 842 993.
 843
 844 Pascotto, M.C., 2006. Avifauna dispersora de sementes de *Alchornea glandulosa*
 845 (Euphorbiaceae) em uma área de mata ciliar no estado de São Paulo. *Revista*
 846 *Brasileira de Ornithologia* 14, 291-296.

847

848 Pinheiro, J., Bates, D., DebRoy, S., Sarkar, D., Core Team, R. 2017. nlme: Linear and
849 nonlinear mixed effects models. R Package Version, 3.1–131.

850

851 Quentin, A.G., Crous, K.Y., Barton, C.V.M., Ellsworth, D.S, 2013. Photosynthetic
852 enhancement by elevated CO₂ depends on seasonal temperatures for warmed and non-
853 warmed *Eucalyptus globulus* trees. Tree Physiology 35, 1249-1263.

854

855 Robakowski, P., Li, Y., Reich, P.B. 2012. Local ecotypic and species range-related
856 adaptation influence photosynthetic temperature optima in deciduous broadleaved
857 trees. Plant Ecol. 213, 113-125.

858

859 Rodrigues, R.R., Lima, R.A.F., Gandolfi, S., Nave, A.G., 2009. On the restoration of
860 high diversity forests: 30 years of experience in the Brazilian Atlantic Forest. Biol.
861 Conserv. 142, 1242-1251.

862

863 Russo, S., Sillmann, J., Fischer, E.M., 2015. Top ten European heatwaves since 1950
864 and their occurrence in the coming decades. Env. Res. Lett. 10, 124003.

865

866 Saxe, H., Ellsworth, D.S., Heath, J., 1998. Tree and forest functioning in an enriched
867 CO₂ atmosphere. New Phytol., 139, 395-436.

868

869 Siebke, K., Ghannoum, O., Conroy, J.P., von Caemmerer, S., 2002. Elevated CO₂
870 increases the leaf temperature of two glasshouse-grown C₄ grasses. Funct. Plant Biol.
871 29, 1377-1385.

872

873 Šigut, L., Holířová, P., Klem, K., Šprtová M., Calfapietra, C., Marek, M.V., Špunda,
874 V., 2015. Does long-term cultivation of sapling under elevated CO₂ concentration
875 influence their photosynthetic response to temperature? *Ann. Bot.* 166, 929-939.

876

877 Slot, M., Garcia, M.N., Winter, K., 2016. Temperature response of CO₂ exchange in
878 three tropical tree species. *Funct. Plant Biol.* 43, 468-478.

879

880 Slot, M., Winter, K., 2017a. In situ temperature relationships of biochemical and
881 stomatal controls of photosynthesis in four lowland tropical tree species. *Plant Cell*
882 *Env.* 40, 3055-3068.

883

884 Slot, M., Winter, K., 2017b. Photosynthetic acclimation to warming in tropical forest
885 tree seedlings. *J. Exp. Bot.* 68, 2275-2284.

886

887 Slot, M., Winter, K., 2017c. In situ temperature response of photosynthesis of 42 tree
888 and liana species in the canopy of two Panamanian lowland tropical forests with
889 contrasting rainfall regimes. *New Phytol.* 214, 1103-1117.

890

891 UNFCCC (2015) Adoption of the Paris Agreement, 21st Conference of Parties, Paris,
892 United Nations.

893

894 Urban, J., Ingwers, M.W., McGuire, M.A., Teskey, R.O., 2017. Increase in leaf
895 temperature opens stomata and decouples net photosynthesis from stomatal

896 conductance in *Pinus taeda* and *Populus deltoides* x *nigra*. *J. Exp. Bot.* 68, 1757-
897 1767.

898

899 Vargas, G.G., Cordero R.A.S. 2013. Photosynthetic responses to temperature of two
900 tropical rainforest tree species from Costa Rica. *Trees*, 27, 1261-1270.

901

902 Vårhammar, A., Wallin, G., McLean, C.M., Dusenge, M.E., Medlyn, B.E., Hasper,
903 T.B., Nsabimana, D., Uddling, J., 2015. *New Phytol.* 206, 1000-1012.

904

905 Wahidah, M.N.L., Juliana, W.A.W., Nizam, M.S., Radziah, C.M.Z.C., 2017. Effects
906 of elevated atmospheric CO₂ on photosynthesis, growth and biomass in *Shorea*
907 *platycarpa* F. Heim (Meranti Paya). *Sains Malaysiana* 46, 1421-1428.

908

909 Warren, J.M., Norby, R.J., Wullschleger, S.D., 2011. Elevated CO₂ enhances leaf
910 senescence during extreme drought in a temperate forest. *Tree Physiol.* 31, 117-130.

911

912 Way, D.A., Oren, R., Kroner, Y., 2015. The space-time continuum: the effects of
913 elevated CO₂ and temperature and the importance of scaling. *Plant Cell Env.* 38, 991-
914 1007.

915

916 Wertin, T.M., McGuire, M.A., Teskey, R.O., 2010. The influence of elevated
917 temperature, elevated atmospheric CO₂ concentration and water stress on net
918 photosynthesis of loblolly pine (*Pinus taeda* L.) at northern, central and southern sites
919 in its native range. *Glob. Change Biol.* 16, 2089-2103.

920

921 Yamori, W., Hikosaka, K., Way, D.A., 2014. Temperature response of photosynthesis
922 in C₃, C₄, and CAM plants: temperature acclimation and temperature adaptation.
923 Photosynth. Res. 199, 101-117.
924
925 Yepes Mayorga, A. 2010. Desenvolvimento e efeito da concentração atmosférica de
926 CO₂ e da temperatura em plantas juvenis de *Hymenaea courbaril* L., jatobá. PhD
927 thesis, Universidade de São Paulo, São Paulo.
928
929

930 Tables

931 Table 1. ANOVA results for stomatal conductance linear mixed effects model.

932 Temperature and CO₂ refer to treatment effects. Asterisks denote *P* values: *** *P* <

933 0.0001, ** *P* < 0.001, * *P* < 0.05, • *P* < 0.1, ns not significant.

Model Term	Numerator DF	Denominator DF	F
Intercept	1	551	213.0***
Time	1	551	48.3***
Time ²	1	551	204.3***
PAR	1	551	28.5***
<i>D</i>	1	551	0.17 ^{ns}
Temperature	1	28	15.7**
CO ₂	1	28	3.2•
Temperature: <i>D</i>	1	551	6.5*
CO ₂ : <i>D</i>	1	551	2.3 ^{ns}
Temperature:CO ₂	1	28	1.3 ^{ns}
Temperature:CO ₂ : <i>D</i>	1	551	16.7**

934

935 Table 2. ANOVA results for *A-T_L* linear mixed effects model. CO₂ refers to treatment.

936 Asterisks denote *P* values: *** *P* < 0.0001, ** *P* < 0.001.

Model Term	Numerator DF	Denominator DF	F
Intercept	1	91	421.9***
Leaf Temperature	1	91	66.9***
CO ₂	1	10	14.7*
Leaf Temperature:CO ₂	1	91	11.8**

937

Table 3. Parameter estimates of Arrhenius functions of the temperature sensitivity of V_{cmax} and J_{max} . Standard errors are given in brackets. Significance of between treatment effects are shown: * $P < 0.05$, • $P < 0.1$, ns not significant. Letters denote differences between treatments.

Chamber	V_{cmax25}	$E_a (V_{cmax})$	J_{max25}	$E_a (J_{max})$
aTaC	13.8 (2.74) AB	81702 (16778) AB	24.95 (1.14)	32187 (4279)
eTaC	14.2 (1.27) A	80644 (7551) A	24.0 (1.84)	27499 (7183)
aTeC	11.0 (1.75) AB	71004 (13689) AB	-	-
eTeC	10.5 (0.26) B	62050 (2171) B	21.8 (3.35)	25840 (14184)
Among Chambers	*	•	ns	ns

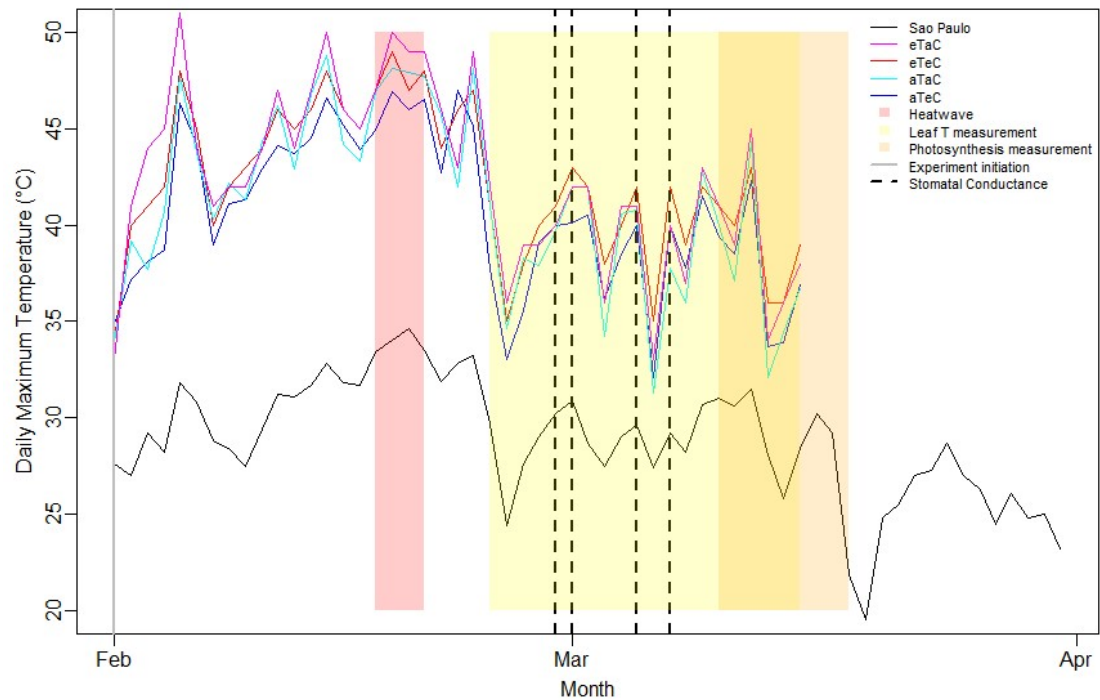


Figure 1. Time series of daily maximum temperatures in São Paulo (Mirante de Santana weather station, data from INMET, <http://www.inmet.gov.br/portal/>, accessed 22/05/2018) and in each experimental chamber during the experiment. The experiment was initiated on 1 Feb 2017. The period classified as a heatwave, periods of leaf temperature and photosynthesis data collection, and days in which diurnal cycles of stomatal conductance were performed are shown.

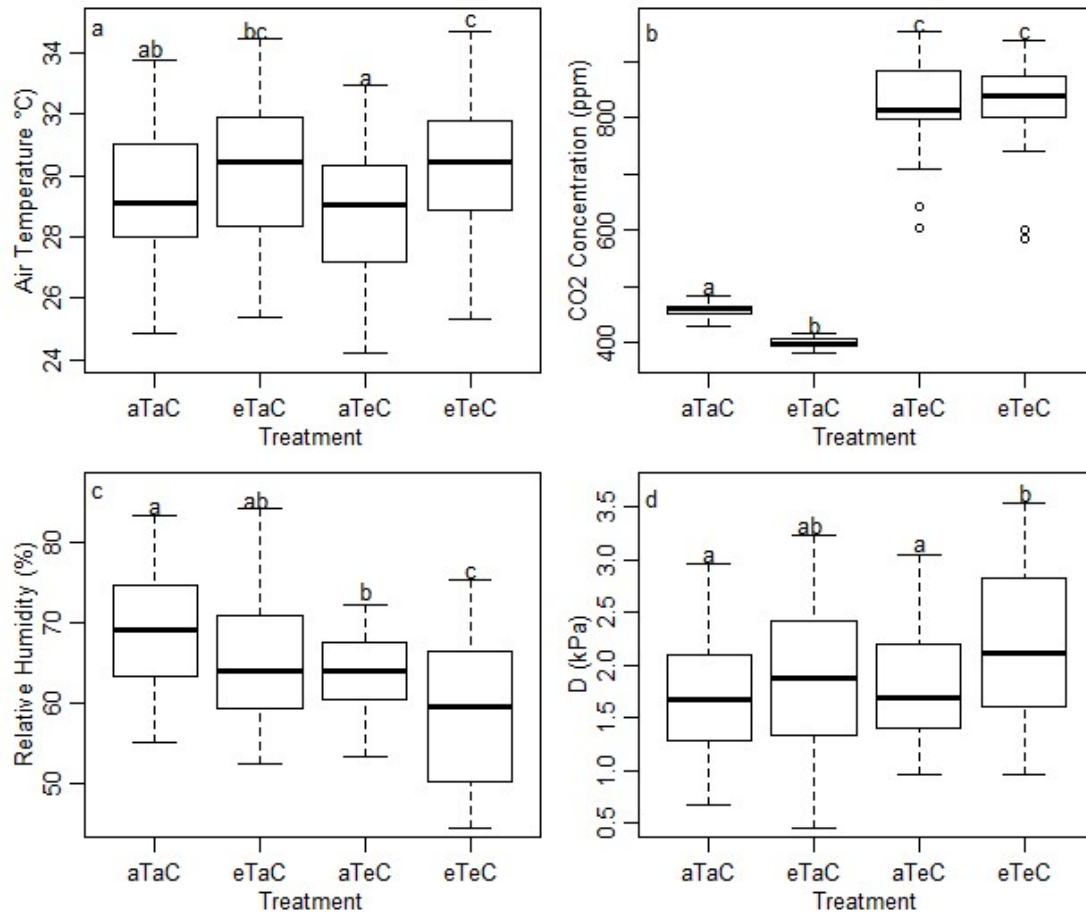


Figure 2. Differences in microclimate variables between chambers a) mean air temperature, b) mean CO₂ concentration, c) mean relative humidity, d) mean *D*. Box plots show daily averaged values from both the acclimation and measurement periods. Treatments: aTaC – ambient temperature and CO₂, eTaC – elevated temperature and ambient CO₂, aTeC – ambient temperature and elevated CO₂, eTeC – elevated temperature and CO₂.

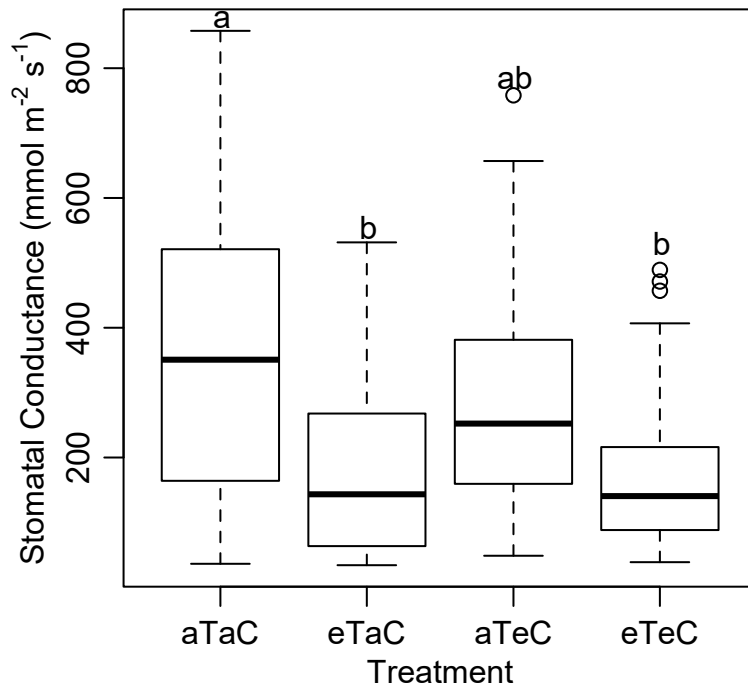


Figure 3. Effect of treatment on stomatal conductance where measurements from all times of day are pooled. Treatments: aTaC – ambient temperature and CO₂, eTaC – elevated temperature and ambient CO₂, aTeC – ambient temperature and elevated CO₂, eTeC – elevated temperature and CO₂.

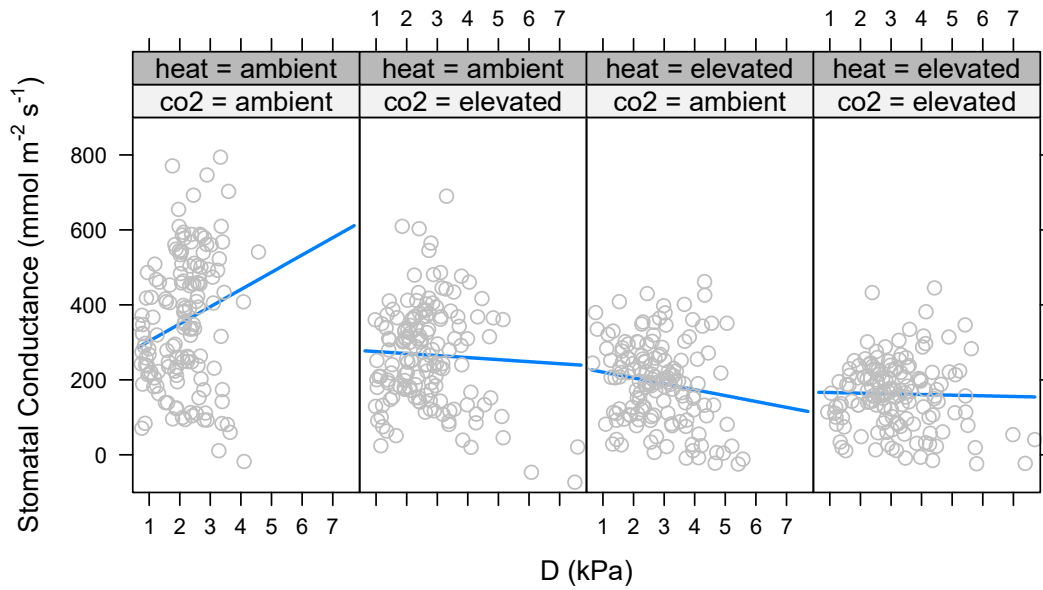


Figure 4. The relationship between g_s and leaf-to-air D for each treatment (accounting for time of day (t , hours) and PAR as fixed effects and leaf as a random factor). Grey points show the partial residuals of the model. Full model equations: $-1053.2 + 215.6 \cdot t - 8.6 \cdot t^2 + 0.13 \cdot \text{PAR} + 45.9 \cdot D$ (aTaC); $-1029.7 + 215.6 \cdot t - 8.6 \cdot t^2 + 0.13 \cdot \text{PAR} - 7.0 \cdot D$ (aTeC); $-1074.1 + 215.6 \cdot t - 8.6 \cdot t^2 + 0.13 \cdot \text{PAR} - 17.3 \cdot D$ (eTaC); $-1142.5 + 215.6 \cdot t - 8.6 \cdot t^2 + 0.13 \cdot \text{PAR} - 2.6 \cdot D$ (eTeC).

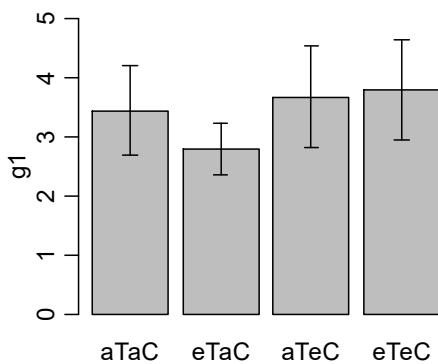
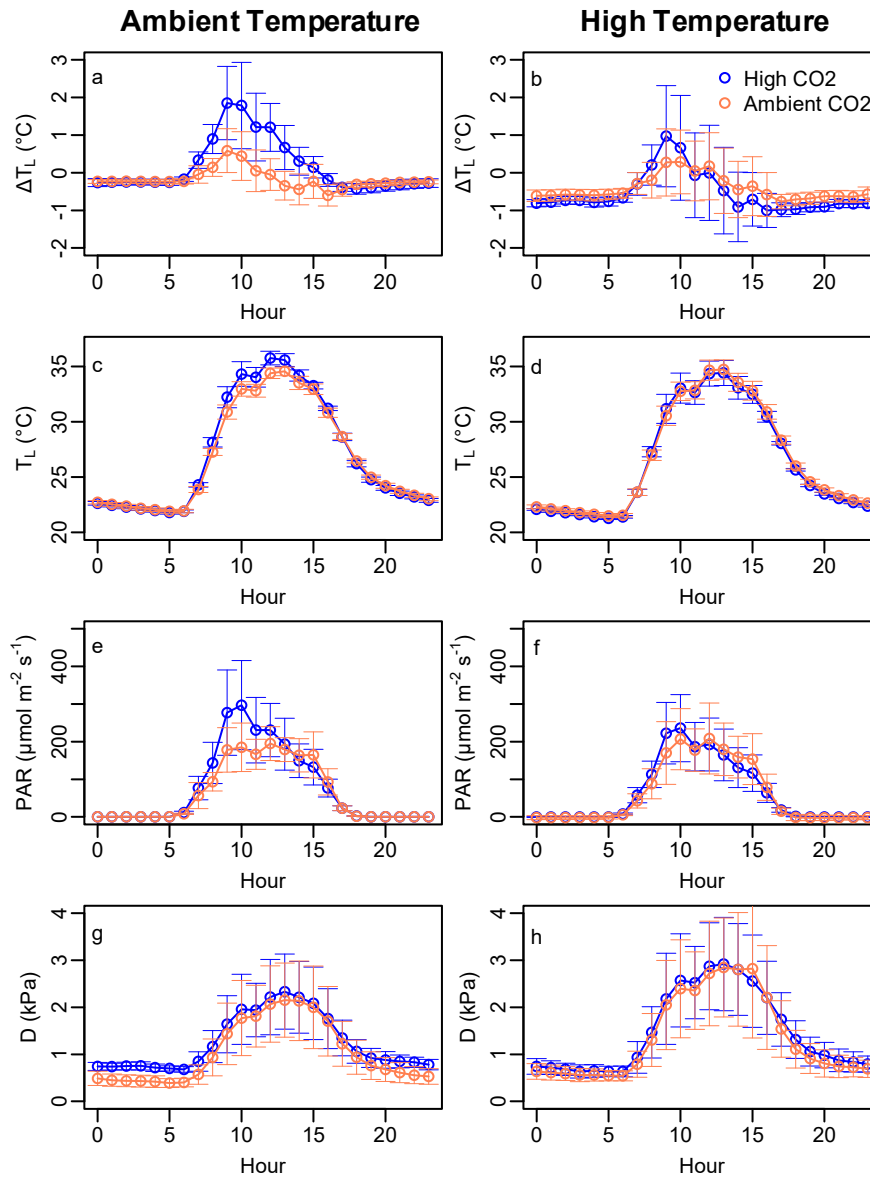


Figure 5. Comparison of the g_1 stomatal conductance parameter (unitless) between chambers. Bars show the mean value and error bars the standard deviation.



980

981 Figure 6. Diurnal cycles of leaf-to-air temperature difference (a,b), leaf temperature

982 (c,d), PAR (e,f), D (g,h), for chambers with ambient air temperature (a,c,e,g) and

983 elevated temperatures (b,d,f,h).

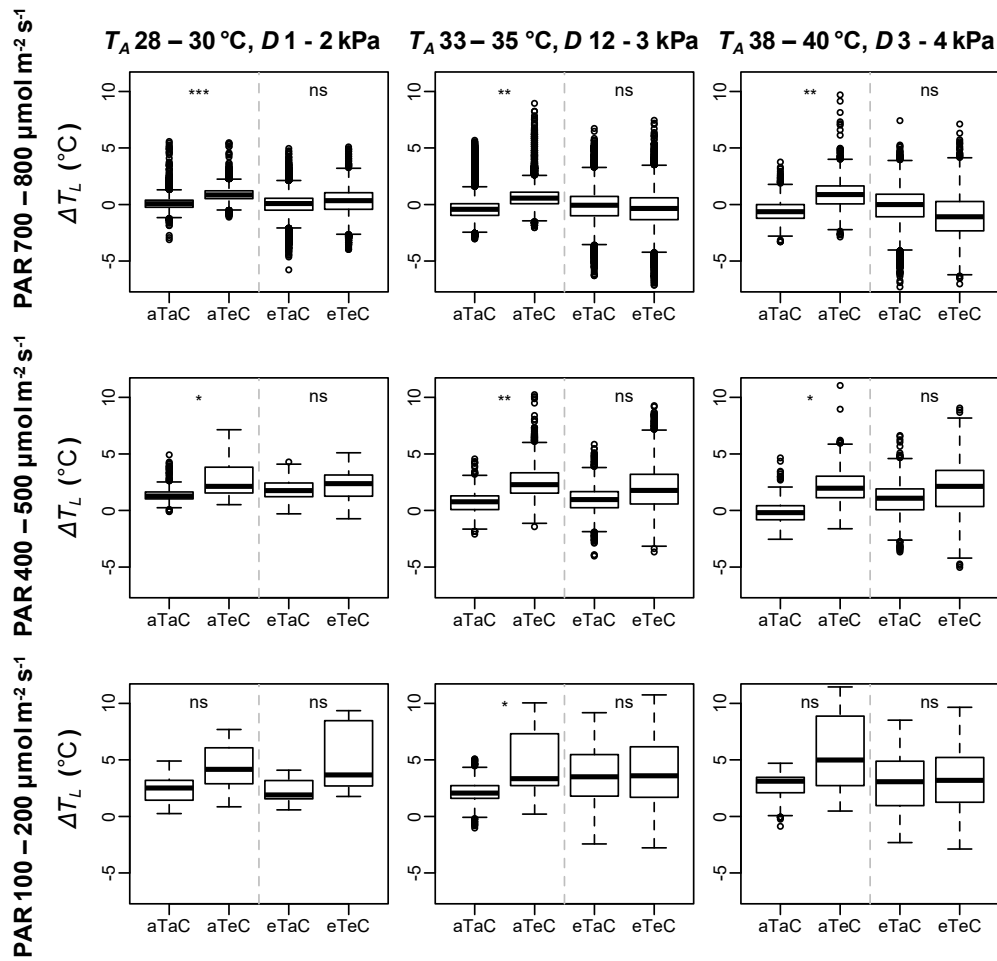


Figure 7. Leaf to air temperature differences for each treatment under a range of microclimate conditions. Contrasts are made between aC and eC under ambient the temperature treatment, and between aC and eC under the elevated temperature treatment, using mixed effects models with leaf as a random factor. Data is from ΔT_L measurements at 10 s temporal resolution subsetted for specific chamber air temperature (T_A) and D conditions, and leaf surface PAR conditions. Asterisks denote P values: *** $P < 0.0001$, ** $P < 0.001$, * $P < 0.05$, ns not significant.

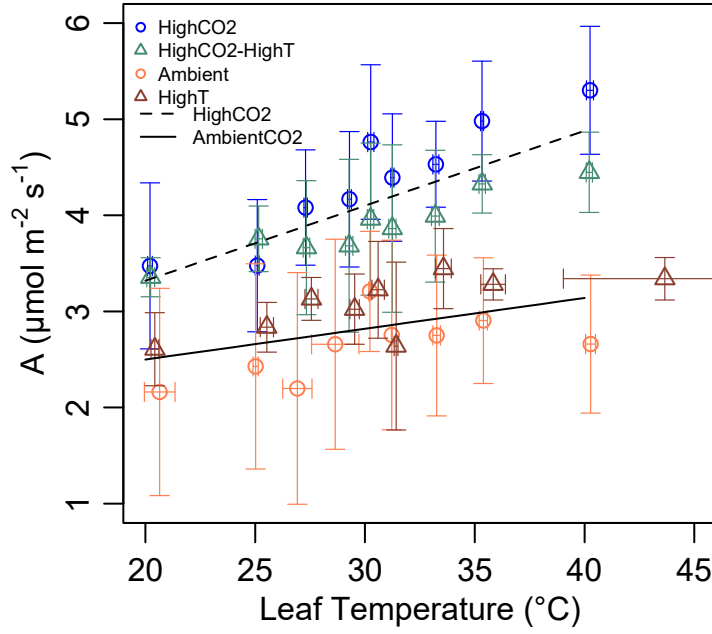


Figure 8. Temperature response of net photosynthesis. Under high CO₂ net photosynthesis is higher and the temperature response is steeper. For ambient CO₂ $A = 1.86 + 0.032 \cdot T_L$; for elevated CO₂ $A = 1.75 + 0.078 \cdot T_L$.

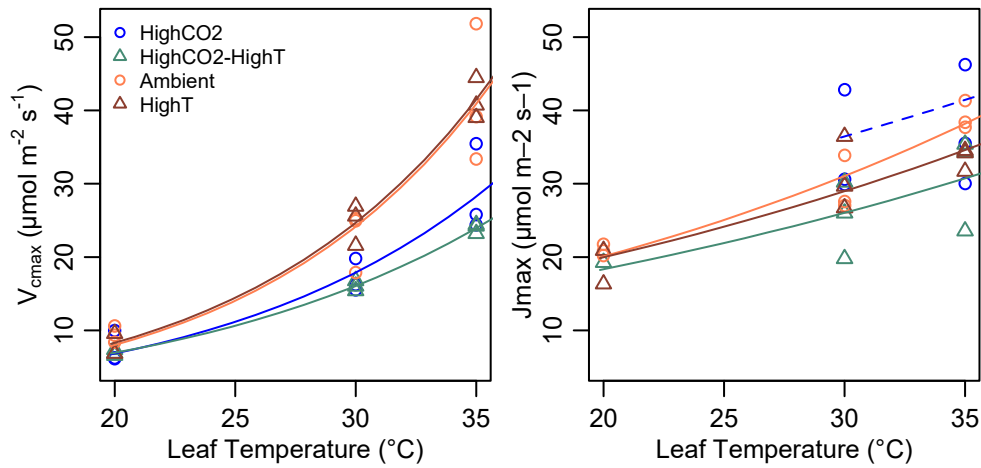


Figure 9. Temperature response of V_{max} and J_{max} fit with Arrhenius functions. For J_{max} in the high CO₂ treatment no values at 20 °C were obtainable. Equation parameters are given in Table 3.